NeuroImage **11,** 167–178 (2000)
doi:10.1006/nimg.1999.0524, available online at http://www.idealibrary.com on IDEAL®

Neuromagnetic Localization of CMV Generators Using Incomplete and Full-Head Biomagnetometer

J. Dammers*,† and A. A. Ioannides‡

*Institute of Medicine Research Centre Jülich, 52425 Jülich, Germany; †Department of Physics, Open University, Milton Keynes MK6 7AA, United Kingdom; and ‡Laboratory for Human Brain Dynamics, Brain Science Institute, RIKEN, Wako-shi 351–01, Japan

Received May 19, 1999

Contingent magnetic variation (CMV) data were recorded in three healthy male subjects using a 2 × 37 biomagnetometer system. The experiment was repeated for one of the subjects using a 151 whole-head biomagnetometer; the same auditory GO/NOGO choice reaction time paradigm as in the first experiment was used, extended to include repetitions of identical runs and additional control conditions. Magnetic field tomography was applied to the averaged data of each subject, for each run and condition (e.g., GO/NOGO). An independent estimate of the current density in the brain was obtained every few milliseconds. The slow components were emphasized by integrating the square of the current density vector, pixel by pixel, revealing in each subject activity in the auditory cortex, sensorimotor cortex, inferior prefrontal area, and posterior inferior parietal area. The intersubject variability was large, but looking across subjects the auditory and sensorimotor cortex (which were best covered by the two probes) were consistently identified in each subject as contributing to the generation of the early and late slow CMV components. These findings were confirmed by the whole-head single-subject experiment, in which slow activity was also identified in the supplementary motor area (SMA) and posterior cingulate cortex (PCC), areas very likely missed in the first experiment because of the limited view of the twin system. The PCC and particularly the SMA activations were substantially reduced when identical runs were repeated.

INTRODUCTION

Although the first report about contingent negative variation (CNV) was published 35 years ago by Walter *et al.* in 1964 there is still considerable uncertainty regarding the neuronal generators of the CNV. In general, the CNV is a surface-negative slow electrical potential generated in the time interval between a warning (S1) and an imperative (S2) stimulus. The activity during the waiting period between the warning and the imperative stimulus differs depending on whether the subject performs (GO) or withholds (NOGO) a movement (Walter *et al.*, 1964). This difference is enhanced when a reward or punishment is given following correct or wrong motor responses, respectively. For many subjects, when the two stimuli are separated by a period of 2 s or more the CNV separates into at least two slow components. The first slow component is referred to as the early CNV, which begins at 300–500 ms after S1 and lasts usually for about 1 s or less. The second slow component, called the late CNV, begins 1.5 to 2 s before S2 and has its maximum 200 to 300 ms prior to S2. Studies with intracranial electrodes, in both man and animals, have demonstrated that multiple cortical and subcortical brain areas are involved in the CNV generation (Nakamura *et al.*, 1988; Ikeda *et al.*, 1995, 1998; Hamano *et al.*, 1997; Lamarche *et al.*, 1995). In these studies, however, only the activity in the very local area where electrodes were placed can be identified.

The magnetic counterpart of the CNV is coined the contingent magnetic variation (CMV). The CMV is a laborious and long experiment, but it was nevertheless studied even with a single channel (Weinberg *et al.*, 1983) and in numerous recent studies with multichannel probes. It is widely accepted that the CMV generators are widely distributed in the brain, a fact which explains the rather limited success in modeling the CMV using only one or a few point-like generators (Elbert *et al.*, 1994). A notable exception is the study of Basile *et al.* (1994) in which a specific frontal activation was observed, but in a protocol which relied on working memory task with space and pattern recognition components.

In all our CMV studies, past and present, we have used distributed source analysis, which has been successfully applied before the identification of either focal or distributed activations. In one of our earlier studies (Ioannides *et al.*, 1994) magnetic field tomography (MFT) analysis identified activity in each of the two subjects studied in the sensorimotor, supplementary

1053-8119/00 $35.00

motor area (SMA), and parietal areas. In addition, a clear priming of the left (contralateral) auditory cortex was observed in the GO condition when the auditory stimuli was delivered to the right ear (Ioannides *et al.*, 1994). In these earlier studies of the CMV we used a single 37-channel probe and hence at any one session either the left or the right temporal areas or the superior parts of the brain could be adequately covered. We investigated all conditions with a centrofrontal dewar location and just one more placement of the single probe (37 channels) over the left lateral area and with a task involving auditory stimuli delivered to the right ear and movement execution or inhibition with the right index finger. Guided by our earlier CMV results (Ioannides *et al.*, 1994; Liu *et al.*, 1996) we have undertaken the current CMV study which is in two parts. In the first part (Experiment 1) we will present results from three subjects who have been investigated using the BTi twin probe MAGNES system. Each 37-channel probe was placed over the left or right auditory cortex; with such a sensor placement reliable estimates of activity could be obtained in the left and right auditory and motor cortices and to a lesser extent in the frontal and parietal areas. In the second part (Experiment 2) of the study one of the three subjects (JD) volunteered for a repetition of the CMV experiment using the CTF Omega 151a whole-cortex system. The three-subject study with the twin probe verified and extended the earlier results, while the single-subject analysis of the whole-head data revealed laterality effects and changes in SMA and posterior cingulate cortex (PCC) activations within the same experimental session.

MATERIAL AND METHODS

Subjects

Five healthy male volunteers (mean age 37.2 ± 8.8; four right handed and one left handed) participated in the MEG experiment in accordance with the Institutional Committee on Human Research. Informed consent was obtained from each volunteer. The data of two subjects were discarded because of unusual large slow-frequency noise in the laboratory's environment at the time of the experiment. The detailed comparison between low-frequency activity across runs and hemispheres was therefore restricted to three of five subjects. None of the remaining three subjects (DB, JD, RB) had performed the CMV experiment before, and hence a detailed demonstration and time for testing was given to all subjects. Subject JD had been a subject in earlier auditory experiments.

Protocol

In Experiment 1 four conditions (left/right ear presentation and left/right index finger (no) movement) divided the long experiment into four runs with intervening pauses, each run lasting for about 11 min. For convenience we will use a four-label code to distinguish between the four different runs: the first index refers to left/right ear presentation and the second index refers to left/right index finger; for example, the combination LR means left ear presentation and right index finger (no) movement. We presented auditory stimuli in blocked conditions but randomly interleaved 30 GO and 30 NOGO trials within each block (ISI 10.8 ± 2 s), in which 1-kHz tones indicated a NOGO and 2-kHz tones a GO condition. Each tone was delivered at 40 dB above the individual hearing threshold. The warning tone S1 was 250 ms, and the imperative stimuli S2 was 270 ms. The separation (onset-to-onset) between S1 and S2 was chosen to be 3.5 s to separate out the early and late CMV components. For the GO condition, a rapid button-press response was required in the time window of S2 to avoid a 250-ms unpleasant tone burst of white noise delivered with 90 dB through the headphones. The subjects were requested to keep their eyes open and to fixate on a cross-hair placed 1 m away. The same protocol was used for the single-subject Experiment 2, in which the only modification was the number of GO and NOGO trials, which were increased to 50 trials. Only two different conditions (LL1, RR1) were used but each was repeated once (LL2, RR2). Five baseline runs were recorded, two before and three after the CMV runs: the first (pre-CMV) and the last (post-CMV) runs were noise measurements with no subject in place. The second and penultimate runs were noise measurements with the subject in place, but with no tones delivered and with no task set. At the end of the CMV runs, and before the first of the two post-CMV noise measurements, the same stimulation as in condition LL run was repeated but without any response required from the subject. We remark that Experiment 2 was performed 2.5 years after Experiment 1, by which time subject JD had participated in five CMV experiments, with the same or very similar protocol as the one used in the two experiments reported here. Any changes in the activity observed with this subject are not therefore attributable to the use of a naive subject or insufficient training.

Data Acquisition

The MEG signal in Experiment 1 was recorded from each of the three subjects using the BTi MAGNES II system; this consists of two dewars, each housing 37 first-order axial gradiometer channels. The experiment was performed in a magnetically shielded room with lateral placement of either probe over the left and the right side of the head (Figs. 1a and 1b). The positioning of each probe was repeated until the channels of each probe captured the positive and negative field extrema associated with the auditory M100 peak. The single-

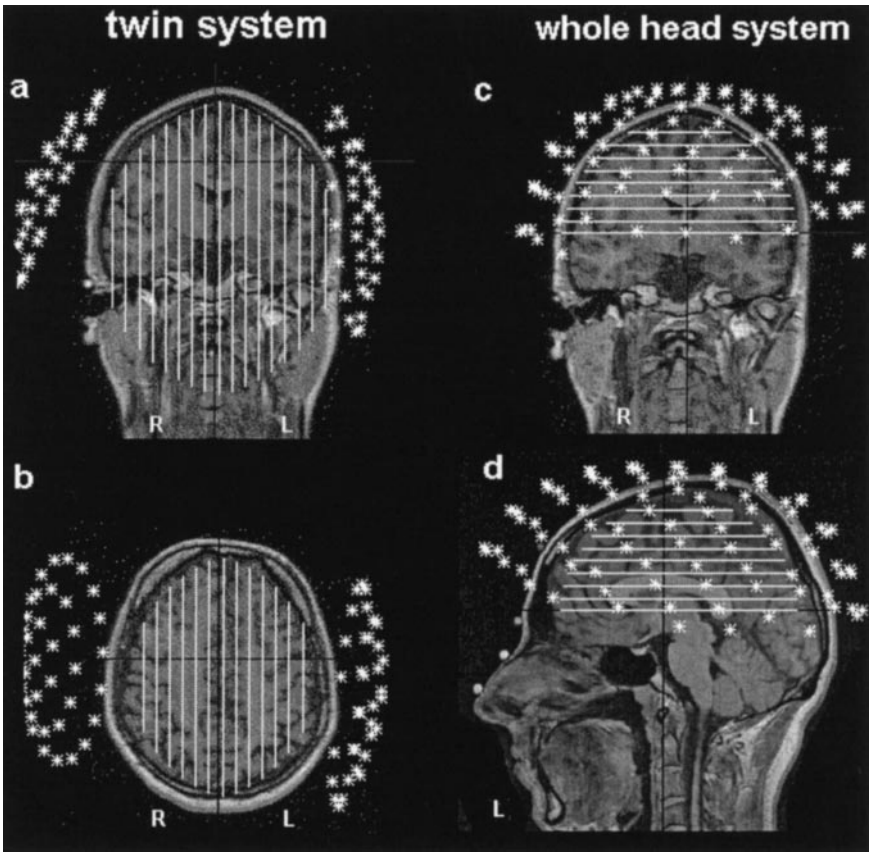

FIG. 1. Channel selection and source space definition. (a and b) The channel layout for Experiment 1 performed with the BTi MAGNES II system and the respective left and right source spaces, used for the MFT reconstructions. Nine sagittal slices are shown for each source space, each appearing as a line in the coronal and axial MRI slices displayed (the deepest slice is common to the left and right source spaces). (c and d) The 90 channels and the top source space used in addition to the lateral source space estimates for the MFT analysis of the helmet MEG data. The coronal and sagittal views are shown, with the nine levels of the top source space cutting the displays at axial planes projected as lines on the display.

subject experiment (Experiment 2) was performed using the CTF Omega 151a whole-cortex system, which consists of a 151 first-order axial gradiometer (Figs. 1c and 1d). Third-order synthetic gradient formation was used to reduce the low-frequency band in the whole-head MEG data (Cheyne *et al.*, 1995). The neuromagnetic activity was continuously recorded with a sampling rate of 1042 Hz and a bandwidth from DC to 400 Hz (Experiment 1) and a sampling rate of 1250 Hz with a bandwidth from DC to 300 Hz (Experiment 2). In all experiments, separate EOG, ECG, and EMG channels were continuously recorded and in synchrony with the MEG channels. A fiber-optic finger movement detection device was used to record the finger movement.

Data Analysis

For further analysis the data were low-pass filtered from DC to 20 Hz to study the slow components as well as band-pass filtered from 3 to 20 Hz for the evoked-like activity. After separation between correct GO and NOGO trials, separate averages were constructed time-locked to both the onset of the warning stimulus (tone averages) and the onset of the TTL signal of the button-press device (button-press averages). The number of trials that remained for averaging in Experiment 1 were (on average) 28.2 ($\pm$1.2) for subject JD, 29.5 ($\pm$0.6) for subject DB, and 26.5 ($\pm$2.3) for subject FB, while in Experiment 2 the number of trials was 33 ($\pm$3.4). MFT, which computes the nonsilent primary current density $J^P(r,t)$ was applied to averaged data separately for the left and right hemisphere to extract time courses of activations (Ioannides *et al.*, 1990). For each hemisphere a separate source space Q (i.e., a 3-D region of space in which $J^P(r,t)$ was allowed to be non-zero) was defined to be a spherical segment that fitted the entire hemisphere (Figs. 1a and 1b). For Experiment 2 an additional top source space was used covering brain areas above the anterior and the posterior commissure (Figs. 1c and 1d). Separate computations were performed for each source space. The reconstructed current densities will be displayed on the background anatomy as gray-level intensity ($P(r,t)$ =

$J^P(r,t)$ [2]). Smoothed integrals of intensity, $A(t,\Delta t)$, in a region of interest (ROI), are defined by

$$A_{\mathrm{ROI}}(t,\Delta t) = \int_{t-\Delta t/2}^{t+\Delta t/2} dt' \int_{\mathrm{ROI}} P(r,t') e^{-(r-r_0^{\mathrm{ROI}})^2/\lambda^2}\, d^3r. \quad (1)$$

Each ROI is bounded by a spherical shell with center at the point r_0^{ROI}; the Gaussian factor controls how points away from the center of the ROI are weighted. In this study we focus on the dynamic of the strongest superficial activations, defined on functional criteria (strongest activity identified by MFT). These functionally defined ROIs were projected onto the individual subject's MRIs. The time course of each ROI was calculated for each subject from separate average signals for each case (LL, RR) computed separately for the GO and NOGO condition as well as for the tone-only case and for the noise runs (averaged in exactly the same way as for the CMV and tone-only presentation cases).

In this study, we will emphasize the slow CNV-type components. These components were difficult to extract because the effectiveness of the passive shielding is greatly reduced, and hence one is more vulnerable to contamination from environmental noise. We will therefore primarily apply MFT analysis to the 0- to 20-Hz data and further amplify the slow components by integrating the intensity as described by Eq. (1) using a running window of 500 ms width. For the reconstructions with lateral dewar placement (Experiment 1) we were forced to use the side source spaces, with separate computations for the left and right hemisphere. For the full-head coverage (Experiment 2) we used 90 sensors in each of three separate reconstructions, two with source spaces identical to those used for Experiment 2 and an additional one using the top source space shown in Fig. 1c. Experiment 2 used MFT estimates obtained with the top source space for all areas, except the auditory cortex, for which we will use MFT estimates obtained with the side source spaces.

RESULTS

As expected we found good agreement in reconstructions obtained from the side and the top source spaces in Experiment 2 when areas were well covered by the sensors in both cases. The evoked-like activity obtained from the 3- to 20-Hz data of Experiment 1 and Experiment 2 reproduced the earlier findings (Ioannides *et al.*, 1994; Liu *et al.*, 1996), in which MFT identified the evoked-like activity in the auditory cortex for all subjects, about 100 ms after the tone onset. In the present study we will restrict attention to the analysis of slow components.

Experiment 1

In all subjects slow CMV-like drifts were identified in the DC to 20-Hz filtered neuromagnetic signals recorded from both left and right hemisphere. Figure 2 shows typical examples of GO and NOGO channels; for each subject a channel above the sensorimotor or parietal area was chosen from the tone-onset-averaged GO and NOGO trials of the first CMV run. A clearly distinguishable slow magnetic field change is evident in the GO trials in all three subjects with a maximum field amplitude varying from 340 to 840 fT among the subjects. The subject-to-subject variability was large but whether this was due to differences in the probe positioning or actual differences in regional brain activ-

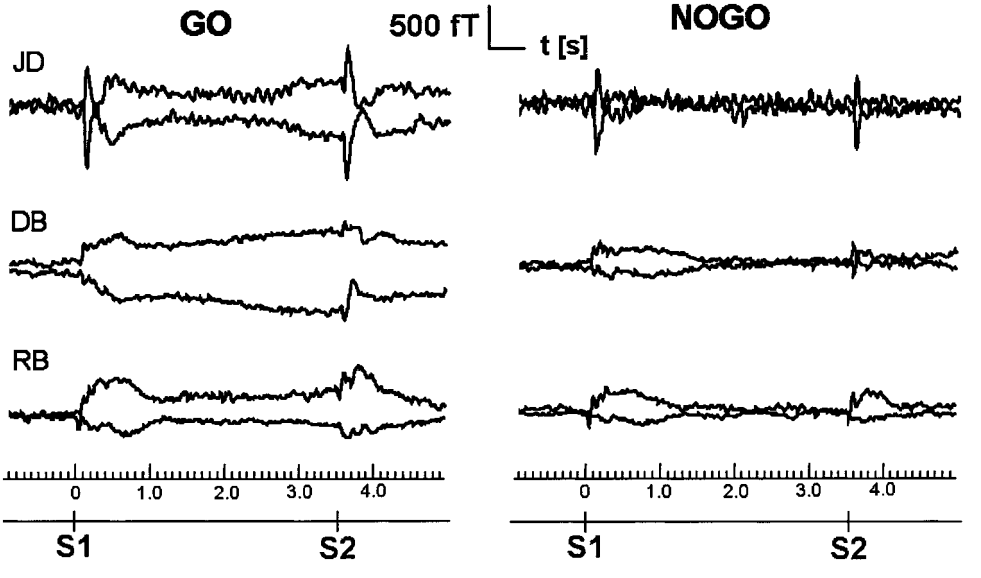

FIG. 2. CMV signal plot for three subjects showing one channel on either hemisphere of the first (tone) averaged CMV run (LL) during GO condition (left) and NOGO condition (right). In each (GO) case the channel with the strongest amplitude is selected.

ity cannot of course be determined by just the morphology of the signals.

MFT analysis of the averaged signals provided the details for the spatiotemporal regional variation (as captured by the averaging process). Activity was identified in the region of the auditory cortex (AC), motor- and sensorimotor cortex (SMC), inferior prefrontal area (IPF), and posterior inferior parietal (PIP) areas (Fig. 5a).

For subject RB, the priming of AC was evident soon after S1 in all four conditions; the AC priming remained high in the GO task. For subject JD the AC priming was again evident in all conditions after S1 but in two conditions (RR, RL) it was reduced to same level as in the NOGO trace. Figures 3a and 3b show the MFT activations of the left and right AC and SMC obtained from the (tone-onset) average DC to 20-Hz signals of the left-handed subject (DB). Figure 3a (SMC ROI) shows a clear late CMV component in all GO task cases, with onset of about 2 s before S2. Figure 3b shows that for this left-handed subject the AC priming after S1 is present in both the ipsilateral and the contralateral side of the brain. The differentiation between the GO and the NOGO conditions is not as clear-cut as for the SMC, but overall the elevated activity remains high through the late CMV in the GO condition.

While the timing of slow activations in the AC and SMC region were broadly consistent across subjects and runs, the ones from the IPF and PIP were highly variable, especially between subjects. It is unclear whether the variability was due to true intersubject differences, reflecting possibly differences in strategy. The within-subject variability can be studied only by a more detailed examination of one subject and with simultaneous recording over all areas. This we have done in the second part of the study.

Figure 4 shows an example of the distribution of MEG signals over the scalp from the second experiment using the whole-head system. The trace for each sensor is plotted for the average signal from the GO condition of the first LL CMV run. The figure shows the characteristic CMV morphology, as already demonstrated in Fig. 2, evident in both hemispheres over the temporoparietal areas, with a stronger slow CMV signal on the contralateral (right) hemisphere. Figure 5 links the two experiments. Figure 5a shows examples of strong instantaneous activations extracted from average MEG data recorded in Experiment 1 (left two columns) and Experiment 2 (right two columns). Activations are displayed at similar but not identical times; the instances displayed were chosen so that the area in question was activated more or less in isolation, at least within the displayed MRI slice. The motor cortex activation is particularly difficult to extract from tone-onset-based average MEG signals. Summing the signal from trials time-locked to the onset of the button press

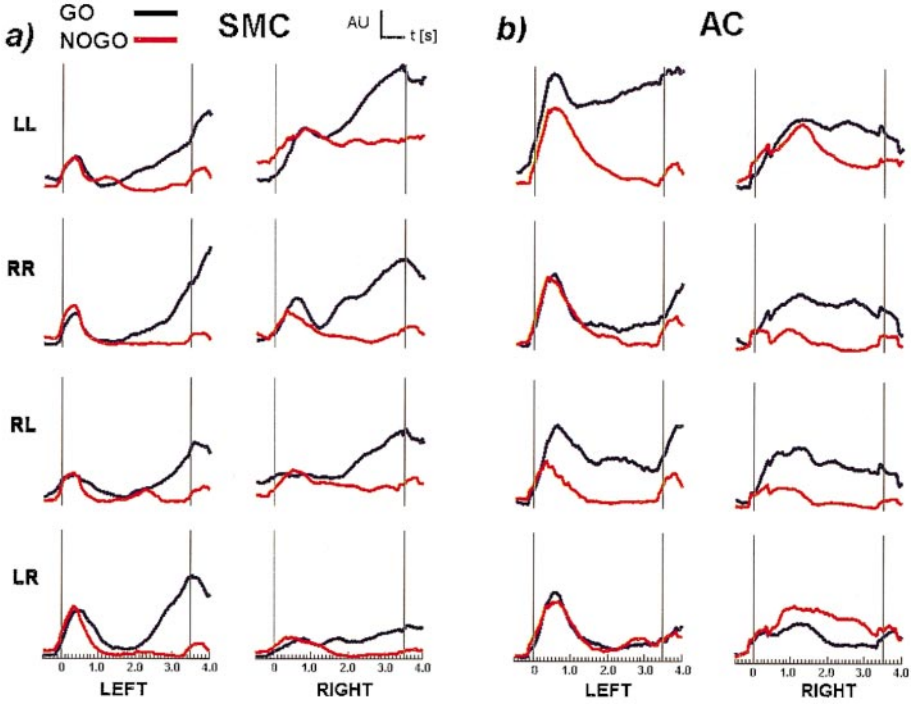

FIG. 3. Time courses of the SMC region (a) and AC region (b) for the left-handed subject DB for the GO (blue line) and NOGO (red line) tone averages of all four conditions. LEFT and RIGHT under the horizontal axes label the source space hemisphere and probe used for the MFT analysis. The first (second) thin vertical line in each graph marks the onset of the warning (imperative) tone. The slow components correspond to integrals of MFT estimates for the modulus of the current density vector over 500 ms.

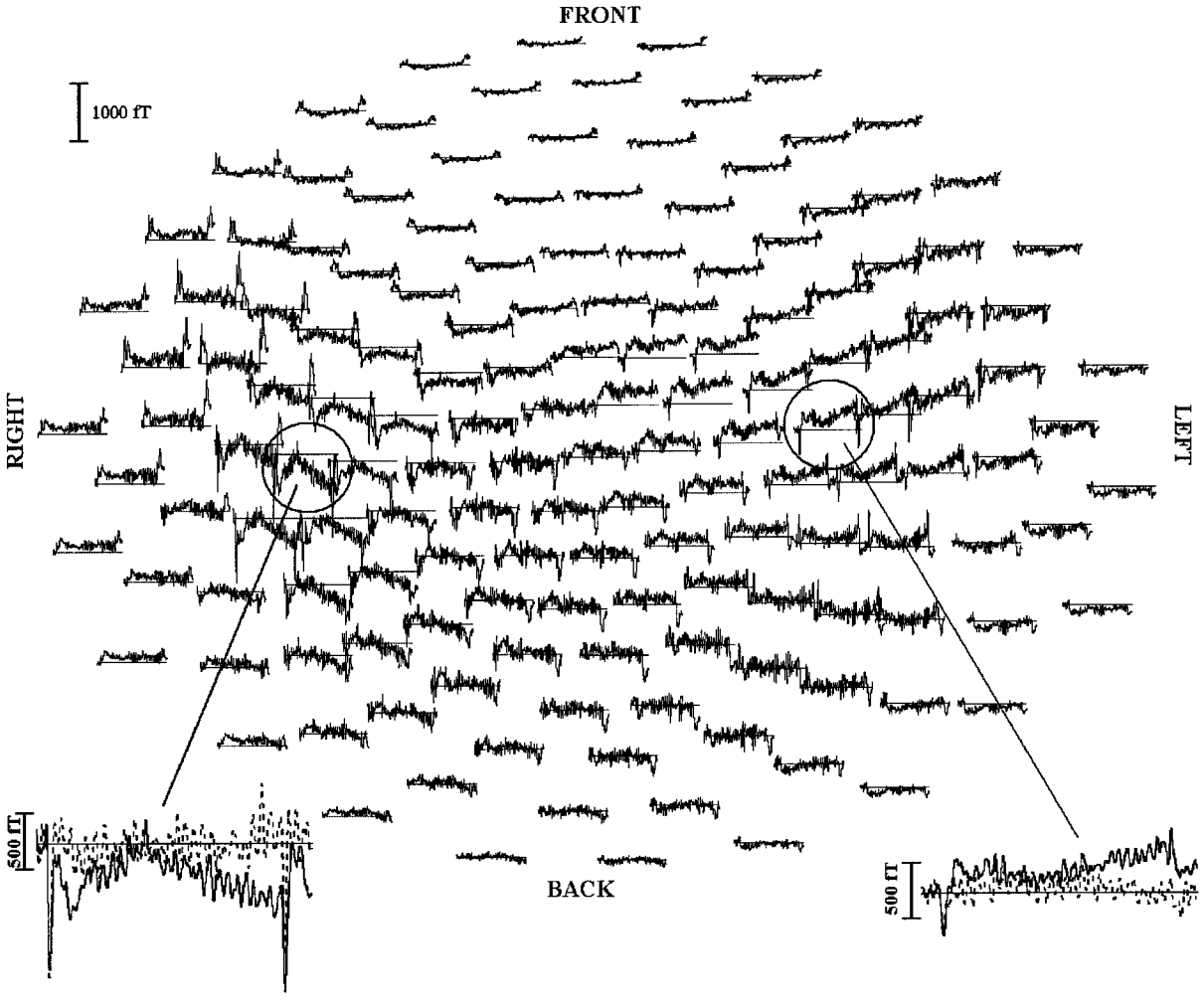

FIG. 4. CMV signal plot of subject JD showing the (tone) average MEG signal (100 ms prestimulus and 4000 ms poststimulus) of the first LL CMV run during GO condition for all 151 sensors. The prominent slow CMV signals are best seen in the temporoparietal areas, with clear enhancement of the contralateral (right) side. One channel on each hemisphere showing the CMV morphology best is highlighted and they are shown in enlargement with the NOGO trace superimposed (dashed).

provides a more appropriate average; the last two images on the right in the second row of Fig. 5a show the SMC MFT estimates from Experiment 2 extracted from the average of single trials filtered in the DC–20 Hz range and time locked to the onset of the button press. The displayed regional activation corresponds to 40 ms before the button press. Figure 5b shows two examples of additional areas seen with the helmet data: the SMA and the PCC. As we will see next the activations in these areas are labile, especially at SMA, where they become weaker when the same run is repeated a few minutes or hours later.

Experiment 2

Figure 6 shows the time courses of the activations in the AC region in the 3–20 Hz filtered range, for the first LL condition. The auditory cortex activation is evident around 100 ms after each tone in all conditions irrespective of task (GO, NOGO, or just tone presentation), and in each of these the activation is much higher than the two "noise" runs. Figure 7 shows the time courses of the reconstructed DC to 20-Hz signal (tone averages) for six areas which have shown up consistently in both experiments. The activations are shown for all CMV conditions (LL1, LL2, RR1, RR2) together with the baseline conditions provided by the tone-only case and the first noise run with subject in place (before the CMV experiment). The activation curves obtained from the AC and SMC ROIs of condition LL1 and RR1 broadly agree with our results from Experiment 1 for the same subject. For the AC, a slow CMV-type component is seen in the right hemisphere, with the early CMV part showing some but not complete differentiation between GO and NOGO conditions. For the SMC, the late component differentiates well between GO and NOGO conditions, especially for the repetition runs. The activ-

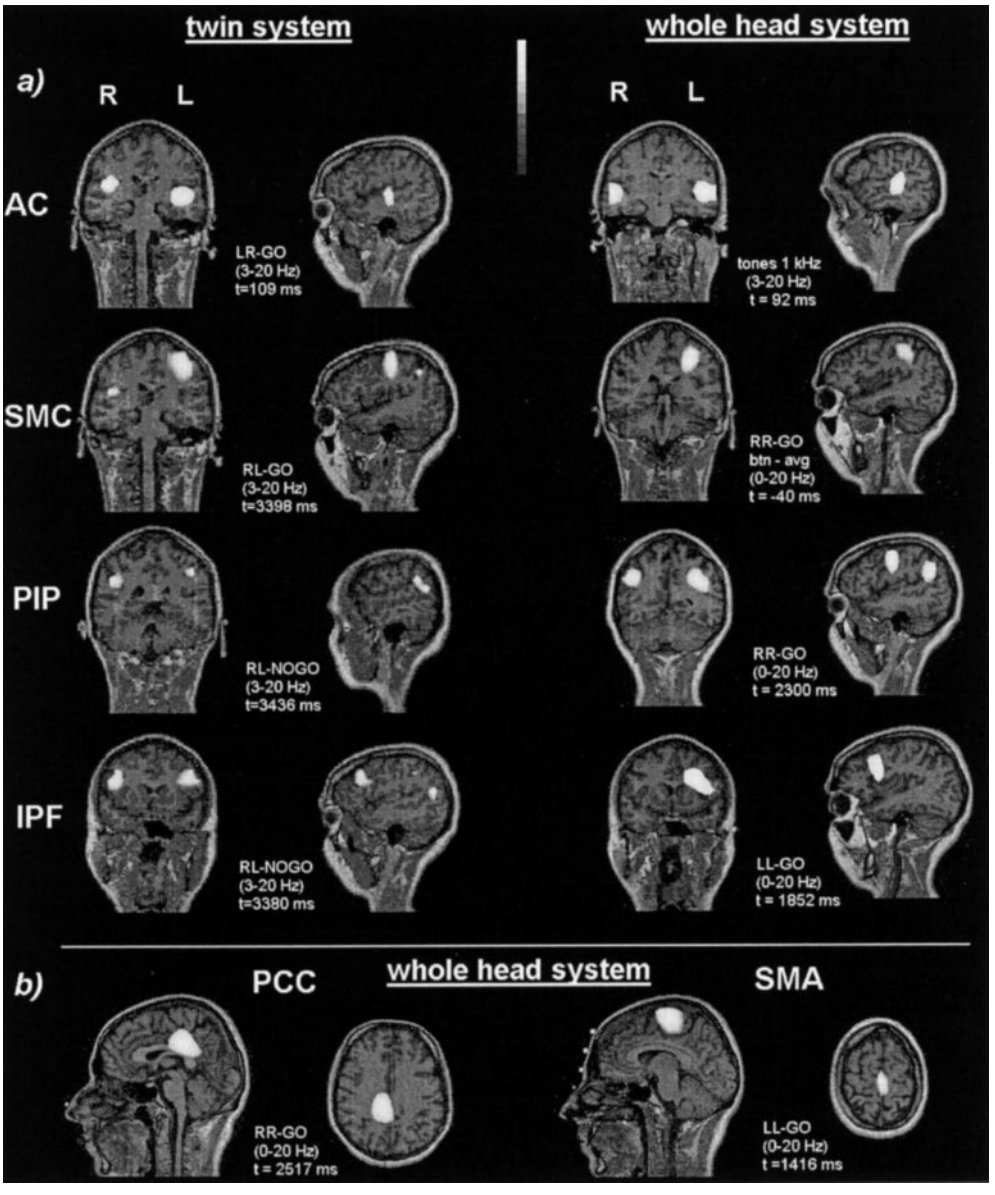

FIG. 5. Instantaneous MFT reconstructions for subject JD, who participated in both experiments. In (a) regional activations are displayed showing in turn from the top: AC, SMC, PIP, and IPF. In each case the activations are superimposed on a coronal and a sagittal slice. The coronal slice is a compromise of the homologous sides on the left and right hemispheres. The displayed areas were identified in all four subjects in Experiment 1 and for JD again in Experiment 2. The display for JD in (a) shows on the left (first two images) MFT reconstructions from the twin MAGNES data (Experiment 1) and on the right (last two images) corresponding MFT reconstructions from the helmet data (Experiment 2).The last row (b) shows two new areas, clearly identified only in Experiment 2, the supplementary motor area (SMA) and the posterior cingulate cortex (PCC). All results are obtained from MFT analysis of the instantaneous value of the average signal at the indicated latency. In all images the averages were computed with single trials aligned to the onset of the tone, except for the whole-head sensorimotor cortex activation (second pair of images on the right), in which the average was performed after aligning the single trials with the onset of the button press.

ity extracted from sensorimotor cortex shows a clear late CMV which is strongest on the left hemisphere (subject JD is right handed). The activation extracted from the tone-only case, which was presented in the same way as the LL condition, shows similar responses compared to NOGO traces (Fig. 7).

In the PIP region a late CMV can be observed in GO traces of all conditions, but on the left hemisphere only, while the right PIP ROI shows priming after S1. Both areas SMA and PCC, which were missed by the sensor arrangement of Experiment 1, are primed in all GO cases of both conditions (LL, RR) starting 200–300 ms after S1. In both hemispheres the SMA (GO-) activity remains high after S1, while a late CMV arises in the

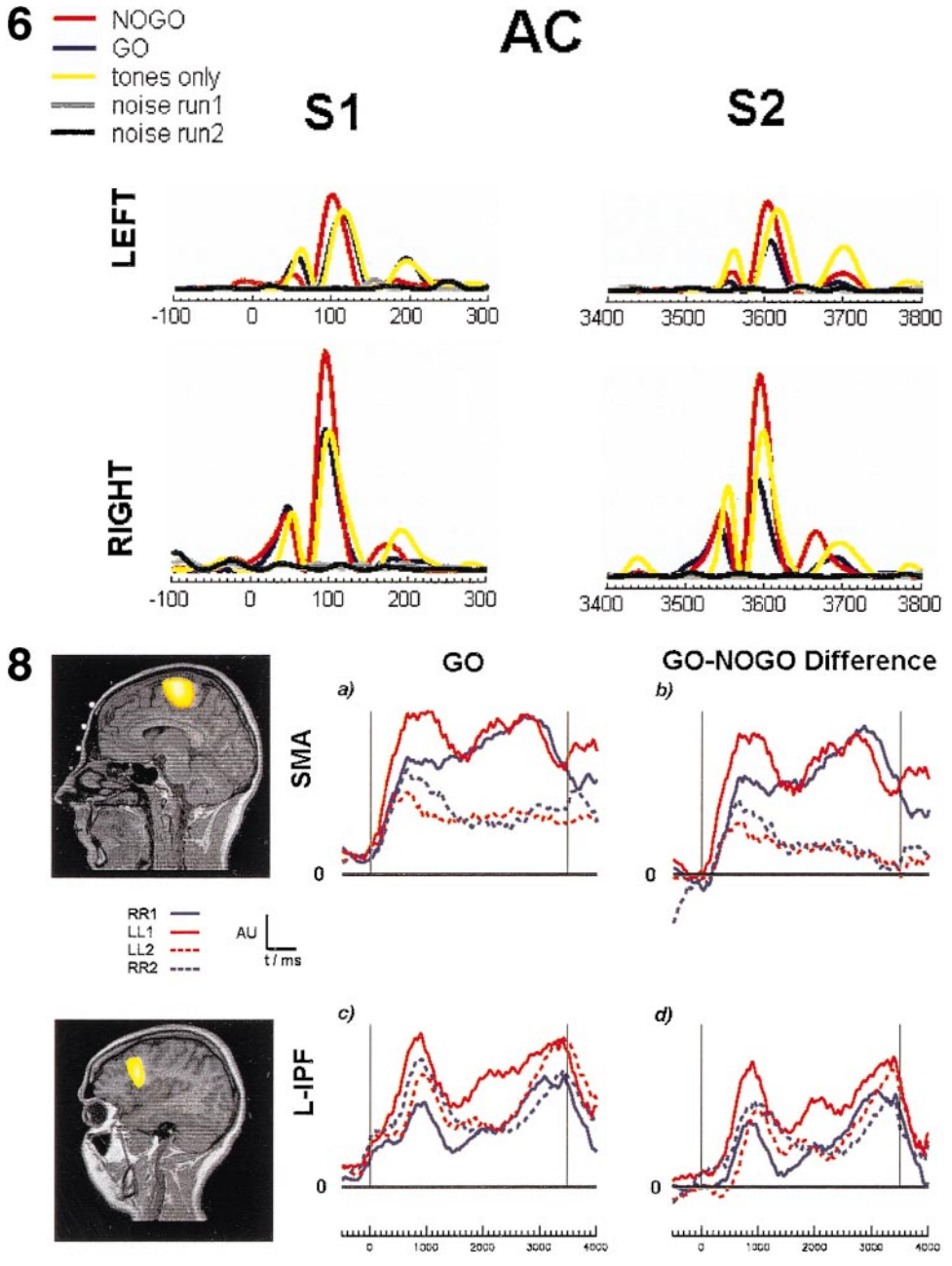

FIG. 6. The evoked-like response in the left and right auditory cortices. Each graph shows the CMV activations (LL1) as blue (GO) and red (NOGO) lines, together with the tone-only condition (yellow line) and the two noise conditions (gray and black lines). In each case the MFT estimates extracted from the 3- to 20-Hz filtered MEG data are displayed for 400 ms showing the square of the current density J, beginning 100 ms before the onset of the tone for both S1 and S2 time periods.

FIG. 8. GO case activations for the SMA (a) and LIPF (b) ROIs in comparison to the difference activation between the GO and the NOGO of the same area. In the case of SMA the mean of the left and right SMA activity is displayed. As in previous figures we have integrated the current density modulus over 500 ms. The sagittal MRI slice of the area is displayed together with the activation of the ROI on its right for the four runs.

PCC region with onset of 2 s before S2. In some ROIs (AC, SMA, PCC) we observe a reduction of slow activity in runs which have been repeated (LL2, RR2). The strongest reduction is obvious in activation of GO traces in the region of SMA and PCC. The most dramatic reduction of the GO to NOGO differential in slow activation between S1 and S2 is in the SMA. The left IPF area produced the most stable and consistently strong activation differentiating the GO and NOGO conditions. The activity in the left IPF decreased rap-

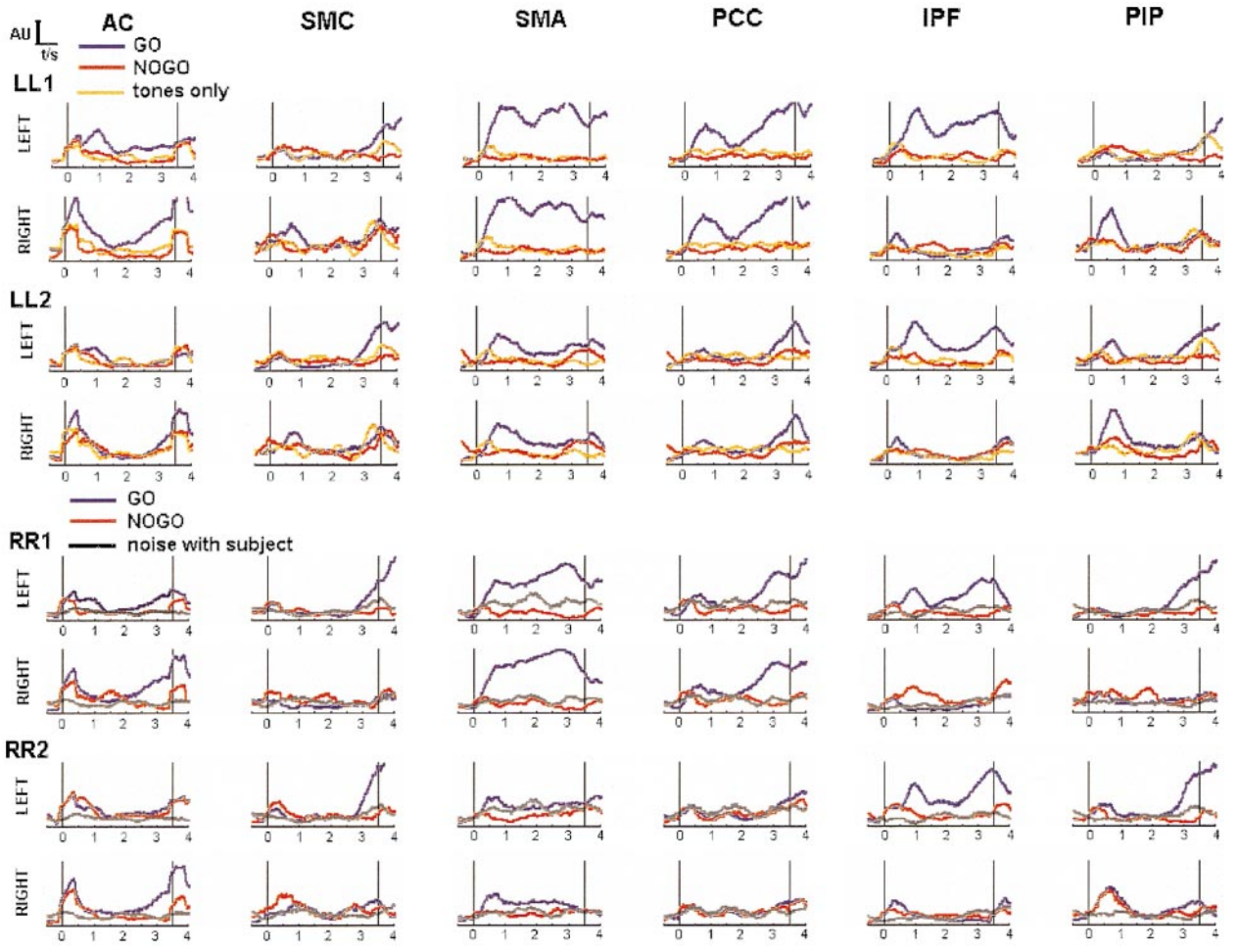

FIG. 7. Time courses of slow regional activations for the AC, SMC, SMA, PCC, IPF, and PIP ROIs, as extracted by MFT analysis of the (tone) average DC to 20-Hz MEG signal from Experiment 2. In each case the instantaneous estimate of the modulus of the current density vector was integrated over 500 ms. In each graph of the top four rows (LL1 and LL2 runs) the traces from the GO (blue) and NOGO (red) are superimposed together with the trace from the tone-only run (yellow), which followed the CMV runs. The SMA and PCC ROIs on the left and right are very similar. In the bottom four rows (RR1 and RR2 runs) the traces from the GO (blue) and NOGO (red) are superimposed together with the trace from the last noise run with subject in place (black), which followed the tone-only run.

idly with the onset of S2. This is the area closest to Sasaki's NOGO area, in terms of both location and function. Figure 8 shows slow activations extracted from GO cases (Figs. 7a and 7c) and the difference between GO and NOGO activations (Figs. 7b and 7d) for the SMA and left IPF region, with the trace of different CMV runs superimposed for each area. In the case of SMA the mean of the left and right SMA activity is displayed. The comparison of the GO activity and the difference between GO and NOGO activity shows that in both areas the proportion of the NOGO activity is negligible.

DISCUSSION

In both experiments we have identified the large slow components that one associates with the CMV protocol. In Experiment 1 the variability across subjects was very large, especially in the wide band filtered data (0–200 Hz). The slow CMV components were best seen when the activity extracted by MFT from the DC to 20-Hz data was integrated over 500 ms. This integration produced stable and largely reproducible activations. In view of our findings during repetitions of identical runs the considerable variability between subjects which still persisted is unlikely to be just noise, but it may reflect a combination of innate differences in the way function is organized in different individuals, different strategies adopted, and training effects, which even for our extensively trained subject JD were clearly in evidence (e.g., SMA activation across repetitions in Fig. 8). This view is supported by the findings of invasive studies (Lamarche *et al.*, 1995), in which it is found that "the slow potentials recorded in the CNV paradigm were of variable shape, preventing a very systematic classification." Nevertheless, for all

subjects and runs free of large low-frequency external noise the slow components were consistently identified in the same areas; the variability was primarily in the timing and duration of slow CNV-like activations in the different areas. In summary, Experiment 1, with coverage over the left and right hemispheres, identified strong contributions from the auditory cortex and sensorimotor cortex to the early and late CMV, in agreement with our earlier findings (Ioannides *et al.*, 1994): In general terms the AC is primed soon after S1 onset as part of the early CMV complex, while the SMC is primed before S2 (as part of the late CMV complex). A slow rise in the AC activity can be seen in both GO and NOGO immediately after S1, but it extends to the late CMV in the GO condition for some, but not all, of the runs and subjects. Activations of IPF and inferior parietal areas was identified in all subjects, but at varied latencies.

Restricting attention to activations from one subject increased the consistency of slow CMV-like components across runs, as shown in Fig. 3 for one of the left-handed subjects. Experiment 2, using a full-head biomagnetometer, pursued the single-subject approach, and the introduction of baseline control conditions and repetitions provided a firmer foundation for the analysis. The specificity of regional activations observed in Experiment 1 was confirmed as expected in the findings of Experiment 2 (e.g., Fig. 5a). The wider sensor coverage showed clearly the contributions to the early and late CMV from the IPF and PIP region and revealed activations in new areas, the SMA and PCC. The absence of these activations from the analysis of data from Experiment 1 is not surprising, because of the unfavorable sensor coverage.

The key role of prefrontal cortex in the CMV generation in general and inhibition of movement has been documented in studies with animals (Sasaki *et al.*, 1989) and humans, in studies with normal subjects (Gemba and Sasaki, 1989) as well as in comparisons between normals and patients (Rosahl and Knight, 1995). Evidence for modulation of the CNV by lateral parietal areas was also provided by human studies (Gemba and Sasaki, 1989; Rosahl and Knight, 1995). Animal experiments provide evidence that well-segregated very focal areas are involved: Sasaki and colleagues, for example, identified focal bilateral areas in the principal sulcus of monkey which are preferentially activated by the NOGO stimuli (Sasaki *et al.*, 1989); the electrical stimulation of these areas during the GO condition delivered at the latencies of the peak of "NOGO" activations produced not only movement suppression but also delay in the execution of movement by a few hundreds of milliseconds (Sasaki *et al.*, 1989). In contrast EEG studies from the scalp show widespread potentials in frontal and parietal areas (Gemba and Sasaki, 1989, Rosahl and Knight, 1995). The focal nature of the activations is, however, confirmed in the intracranial studies (Ikeda *et al.*, 1995, 1996; Hamano *et al.*, 1997; Lamarche *et al.*, 1995). These studies further demonstrated that there are many focal areas which become active when a CNV protocol is used. These studies show also not only that the activation pattern varies between subjects, but also that small changes in the CNV protocol can introduce large changes in the activations. This last point makes it hard to relate the excellent fMRI study of Konishi *et al.* (1998) with the rest of the vast literature of human CNV studies. Konishi *et al.* used fMRI and a long IS interval which allowed them to bin and to study the GO and NOGO trials separately. Unfortunately the protocol did not include a proper warning stimulus, and the analysis was therefore restricted to the time after the imperative stimulus. Nevertheless the clear finding of a right hemisphere IPF focal activation in the NOGO responses is significant and must be eventually understood together with the results reported in our paper and others' findings. Given these complications we decided to explore how the CMV is generated and how it changes in time, by studying in detail one subject. We had already demonstrated in our earlier studies (Ioannides *et al.*, 1994; Liu *et al.*, 1996) the feasibility of identifying focal activations from MEG data of a single subject (even in single trial) using MFT. This liberates us from the constraints of assuming focal activations a priori and relies on the data of each time slice to dictate the number and nature of the strongest generators of the observed signal (Taylor *et al.*, 1999).

For the single-subject study the left inferior prefrontal area was consistently activated in all runs, starting soon after S1 with an early CMV peaked at 900 ms and followed by a late CMV with onset of 1.5–2 s before S2. During the interval between S1 and S2 the early and late CMV-like activation was evident in this area, showing best as the difference between the GO and the NOGO activations. The pattern is consistent with an inhibitory role, as its activity decreases immediately with onset of S2, possibly to allow the execution of the movement. The early activation, coming soon after the auditory- and motor-related areas have completed evoked-like responses to the warning stimulus, is also consistent with a combination of immediate inhibitory function coupled to holding of information regarding the impending movement (the activity is much stronger in the GO condition).

The present study shows that during the GO task strong activity is evident in the supplementary motor area and posterior cingulate cortex. This is in contrast to previous MEG/EEG studies which concluded that symmetrical SMA activation should result in a considerable cancellation of their fields (Bötzel *et al.*, 1993; Nagamine *et al.*, 1996). In this study, the bilateral SMA response was identified from the top and the side MFT

analysis (with 90 sensors each time). These observations agree with findings from studies using implanted intracranial electrodes (Ikeda *et al.*, 1996; Hamano *et al.*, 1997). Particularly in GO cases the SMA activity increases 200–300 ms after S1, which is well over 3 s before any movement has to be made, but this is where the movement-planning stage begins. In terms of latency this agrees with our earlier findings (Liu *et al.*, 1996). The new twist added in the present analysis is the lability of the SMA and PCC activations. Even for the highly trained subject JD, a repetition of the task leads to the same latency for the early CMV component, but a marked reduction in amplitude and an almost elimination of the late component. This high lability of the SMA activation is consistent with numerous animal experiments in which SMA plasticity is demonstrated (Tanji, 1994).

In summary, our work adds to the evidence that CMV generators are highly distributed over the human brain, variable from subject to subject, and labile in detail within subjects and that MFT analysis of MEG data can produce very concrete identifications of focal regional activations, including temporal sequencing and a precise statement about which region shows plasticity through modified activations when the experiment is repeated. The specific results reported here apply only to a single subject. Generalizations are suggestive, but they can be made only with confidence after many such studies have been completed. Given the lengthy nature of the experiments and the long analysis such an undertaking is potentially very useful but also formidable.

ACKNOWLEDGMENTS

The first author gratefully acknowledges the support from RIKEN during his stay at the Laboratory for Human Brain Dynamics, Brain Science Institute (BSI) (RIKEN, Japan), where some of the analysis was completed. Both authors thank Professor Karl Zilles and Dr. Klaus Martin Stephan for critically reading the manuscript. We also thank Dr. Huber Preissl from MEG Center, Institute of Medical Psychology and Behavioural Neurobiology (Germany), as well as Mr. Sixtus Lee and Dr. Douglas Cheyne from CTF System, Inc. (Vancouver, Canada) for their support in doing the experiment.

REFERENCES

Basile, L. F. H., Rogers, R. L., Bourbon, T. W., and Papanicolaou, A. C. 1994. Slow magnetic flux from human frontal cortex. *Electroencephalogr. Clin. Neurophysiol.* **90:**157–165.

Bötzel, K., Plendl, H., Paulus, W., and Scherg, M. 1993. Bereitschaftspotential: Is there a contribution of the supplementary motor area? *Electroencephalogr. Clin. Neurophysiol.* **89:**187–196.

Cheyne, D., Vrba, J., Cheung, T., Burbank, M., Weinberg, H., and Lindinger, G. 1995. Source models of slow magnetic fields accompanying movement: Whole cortex measurements using software gradiometers. In *Biomagnetism: Fundamental Research and Clinical Applications* (L. Deecke, C. Baumgartner, and G. Stroink, Eds.), pp. 125–130. Elsevier, Amsterdam.

Elbert, T., Rockstroh, B., Hampson, S., Pantev, C., and Hoke, M. 1994. The magnetic counterpart of the contingent negative variation. *Electroencephalogr. Clin. Neurophysiol.* **92:**262–272.

Gemba, H., and Sasaki, K. 1989. Potential related to no-go reaction of go/no-go hand movement task with color discrimination in human. *Neurosci. Lett.* **101:**263–268.

Hamano, T., Lüders, H. O., Ikeda, A., Collura, T. F., Comair, Y. G., and Shibasaki, H. 1997. The cortical generators of the contingent negative variation in humans: A study with subdural electrodes. *Electroencephalogr. Clin. Neurophysiol.* **97:**257–268.

Howard, R., and Lumsden, J. 1996. A neurophysiological predictor of reoffending in special hospital patients. *Criminal Behav. Mental Health* **6:**147–156.

Ikeda, A., Lüders, H. O., Shibasaki, H., Collura, T. F., Burgess, R. C., Moris, H. H., and Hamano, T. 1995. Movement-related potentials associated with bilateral simultaneous and unilateral movements recorded from human supplementary motor area. *Electroencephalogr. Clin. Neurophysiol.* **95:**323–334.

Ikeda, A., Lüders, H. O., Collura, T. F., Burgess, R. C., Moris, H. H., Hamano, T., and Shibasaki, H. 1996. Subdural potentials at orbitofrontal and mesial prefrontal areas accompanying anticipation and decision making in humans: A comparison with Bereitschaftspotential. *Electroencephalogr. Clin. Neurophysiol.* **98:**206–212.

Ikeda, A., Shibasaki, H., Kaji, R., Terada, K., Nagamine, T., Honda, M., and Kimura, J. 1997. Dissociation between contingent negative variation (CNV) and Bereitschaftspotential (BP) in patients with parkinsonism. *Electroencephalogr. Clin. Neurophysiol.* **102:**142–151.

Ioannides, A. A., Bolton, J. P. R., and Clarke, C. J. S. 1990. Continuous probabilistic solution to the biomagnetic inverse problem. *Inverse Probl.* **6:**523–542.

Ioannides, A. A., Fenwick, P. B. C., Lumsden, J., Liu, M. J., Bamidis, P. D., Squires, K. C., Lawson, D., and Fenton, G. W. 1994. Activation sequence of discrete brain areas during cognitive processes: Results from magnetic field tomography. *Electroencephalogr. Clin. Neurophysiol.* **91:**399–402.

Kawashima, R., Satoh, K., Itoh, H., Ono, S., Furumoto, S., Gotoh, R., Koyama, M., Yoshioka, S., Takahashi, T., Takahashi, K., Yanagisawa, T., and Fukuda, H. 1996. Functional anatomy of GO/NOGO discrimination and response selection—A PET study in man. *Brain Res.* **728:**79–89.

Konishi, S., Nakajima, K., Uchida, I., Sekihara, K., Miyashita, Y. 1998. No-go dominant brain activity in human inferior prefrontal cortex revealed by functional magnetic resonance imaging. *Eur. J. Neurosci.* **10:**1209–1213.

Kristeva, R., Cheyne, D., and Deecke, L. 1991. Neuromagnetic fields accompanying unilateral and bilateral voluntary movements: Topography and analysis of cortical sources. *Electroencephalogr. Clin. Neurophysiol.* **81:**284–298.

Lamarche, M., Louvel, J., Buser, P., and Rektor, I. 1995. Intracerebral recordings of slow potentials in a contingent negative variation paradigm: An exploration in epileptic patients. *Electroencephalogr. Clin. Neurophysiol.* **95:**268–276.

Liu, M. J., Fenwick, P. B. C., Lumsden, J., Lever, C., Stephan, K. M., and Ioannides, A. A. 1996. Averaged and single-trial analysis of cortical activation sequences in movement preparation, initiation and inhibition. *Hum. Brain Mapp.* **4:**254–264.

Nagamine, T., Kajola, M., Salmelin, R., Shibasaki, H., and Hari, R. 1996. Movement-related slow cortical fields and changes of spontaneous MEG- and EEG-brain rhythms. *Electroencephalogr. Clin. Neurophysiol.* **99:**274–286.

Nakamura, M., Ozawa, N., Shinba, T., and Yamamoto, K. 1992. CNV-like potentials on the cortical surface associated with conditioning in head-restrained rats. *Electroencephalogr. Clin. Neurophysiol.* **88:**155–162.

Rosahl, S. K., and Knight, R. T. 1995. Role of prefrontal cortex in generation of the contingent negative variation. *Cereb. Cortex* **2:** 123–134.

Sasaki, K., Gemba, H., and Tsujimoto, T. 1989. Suppression of visually initiated hand movement by simulation of the prefrontal cortex in the monkey. *Brain Res.* **495:**100–107.

Tanji, J. 1994. The supplementary motor area in the cerebral cortex. *Neurosci. Res.* **19:**251–268.

Taylor, J. G., Ioannides, A. A., and Müller-Gärtner, H.-W. 1999. *IEEE Trans. Med. Imag.* **2:**151–163.

Walter, W. G., Copper, R., Aldridge, V. J., McCallum, W. C., and Winter, A. L. 1964. Contingent negative variation: An electric sign of sensori-motor association and expectancy of the human brain. *Nature* **203:**380–384.

Weinberg, H., Brickett, P., Deecke, L., and Boschert, J. 1983. Slow magnetic fields of the brain preceding movements and speech. *Nuovo Cimento* **2D:**495–504.